Experimental Correction of the Axial Shielding Equation

Eugene PAPERNO, Ichiro SASADA, and Kunihisa TASHIRO

***Abstract*—Conventional analytical description of axial shielding for cylindrical shields is based on the assumption that the field reduction inside the shield is due to the demagnetizing field within the equivalent ellipsoid. It seems more reasonable, however, to employ in the axial shielding equation the demagnetizing factor calculated for the equivalent rod because the shields analyzed have the same outer surface as the rod does. In order to support the above idea experimentally, we built and investigated cylindrical shields having different aspect ratios. The permeability of the shielding material was controlled at a number of levels by magnetic shaking. The results obtained show a good agreement between the experimental and new analytical data.**

***Index Terms*—Amorphous Metglas material, axial (longitudinal) shielding equation, demagnetizing factor, cylindrical shields, magnetic anisotropy, magnetic shaking.**

I. Introduction

Analytical description of axial shielding for cylindrical shields (neglecting the effect of the openings or caps) is based on the assumption [1] that the field reduction inside the shield corresponds to the demagnetizing field, H_d^{ell}, within the equivalent ellipsoid having an average relative permeability $m_{equiv} = 4m\,t/D$ (see Fig. 1)

$$H_{ex} - H_{in} = H_d^{ell} = N_d^{ell} H_{in} (m_{equiv} - 1), \tag{1}$$

where H_{ex} is the uniform external field, H_{in} is the field at the shield's center, N_d^{ell} is the demagnetizing factor of the equivalent ellipsoid [1] (see Fig. 2), and m is the relative permeability. According to (1), the axial shielding factor can be estimated as follows

$$S_{ax} = \left.\frac{H_{ex}}{H_{in}}\right|_{\substack{m_{equiv}>>1 \\ t<<D}} = 4N_d^{ell}\frac{m\,t}{D} + 1, \tag{2}$$

$$S_{ax}\Big|_{\substack{m_{equiv}>>1 \\ t<<D}} = 4N_d^{ell} S_t + 1, \quad S_t\Big|_{\substack{m_{equiv}>>1 \\ t<<D}} = \frac{m\,t}{D}, \tag{3}$$

where S_t is the transverse shielding factor [1].

There is some inconsistency in (1)–(3); it seems more reasonable to employ in the above equations the demagnetizing factor of the equivalent rod, N_d^{rod}, [2] (see Fig. 2) rather than N_d^{ell} because the shields analyzed have the same outer surface as the rod does. It is interesting that numerical calculations do support the above idea [3]. On the other hand, (3) was tested in [1], [4] by measuring the S_t / S_{ax} ratio. However, no account was taken in these experiments of the difference between the axial and transverse relative permeabilities, which are related in a nonlinear manner [4] to the corresponding maximum flux densities (see Fig. 2).

It is important, therefore, to test (2) directly by measuring and substituting in (2) the *axial* shielding factor and *axial* relative permeability.

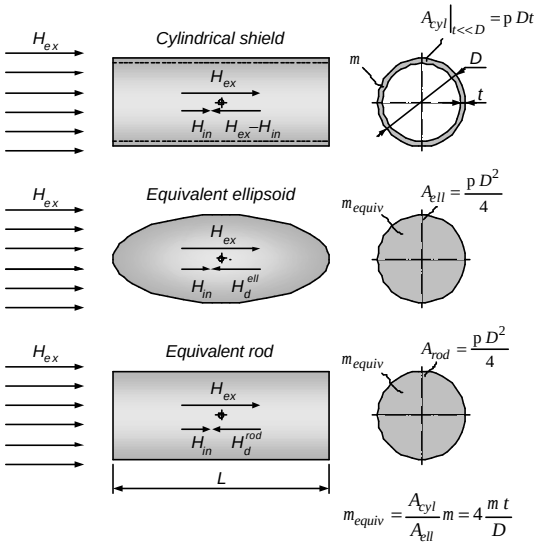

Fig. 1. Magnetic field reduction, H_{ex}-H_{in}, at the center of a cylindrical shield, the equivalent ellipsoid and rod (the effect of the shield openings is neglected).

Manuscript received February 10, 2002.

E. Paperno is with the Department of Electrical and Computer Engineering, Ben-Gurion University of the Negev, P.O. Box 653, Beer-Sheva 84105, Israel (paperno@ee.bgu.ac.il).

I. Sasada and K. Tashiro are with the Department of Applied Science for Electronics and Materials, Kyushu University, Kasuga-koen, Kasuga-shi, Fukuoka 816-850, Japan (sasada@ence.kyushu-u.ac.jp; tashiro@ence.kyushu-u.ac.jp).

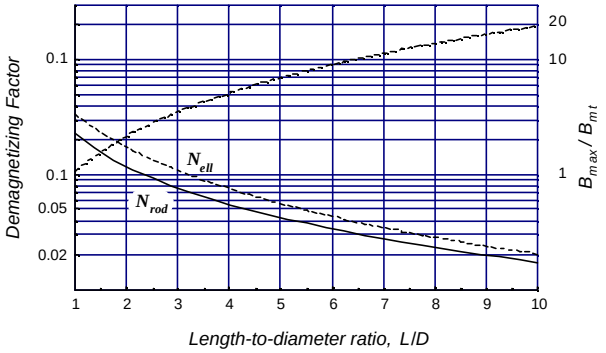

Fig. 2. Demagnetizing factors for ellipsoid and rod as a function of their aspect ratio, *L/D*. Ratio of maximum flux densities in axial and transverse magnetic shields, B_{max}/B_{mt}, as a function of the aspect ratio, *L/D*.

II. Experiment

We used Metglas 2705M amorphous ribbon (see Fig. 3) of 50 mm width and 22 μm thickness, manufactured by Nippon Amorphous Metals, to build the experimental shield models. All shields (see Fig. 4 and Table I) were built by winding 50×50 mm squares cut from the Metglas ribbon around non-conductive pipes in such a way that the magnetic anisotropy direction was in line with the shield axis (see Fig. 3). (We suppose that the air gaps between the ribbons are negligibly thin compared to the ribbon thickness and do not affect the axial shielding factor.) The permeability of the shielding material was controlled at a number of levels by magnetic shaking [5] (see Fig. 4 and Table II).

A special experimental setup was used to measure relative permeability of the shielding material (see Fig. 5, where the applied fields and magnetic anisotropy arrangement imitates the axial shielding in Fig. 4). The permeability measuring procedure was similar to that described in [6]. The conditions and results of this experiment are described in Table II.

We used a miniature magnetoresistive bridge of KMZ10 type, manufactured by Philips, (see Fig. 3) to measure the field at the shields' center. The magnetoresistive bridge was supplied with a 5 V rms, 200 Hz sinusoidal voltage. Such ac bias allowed us to employ synchronous detection of the sensor output. We used an SR830 DSP lock-in amplifier, made by Stanford Research Systems, as the synchronous detector and its internal reference oscillator as the sensor's voltage supply. The total system noise measured at the lock-in amplifier output was about 6 μV/vHz rms that corresponds to a 10 μOe/vHz resolution. The external field frequency was set at

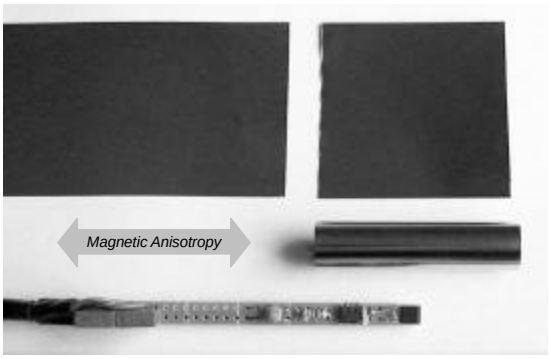

Fig. 3. A miniature shield model made of 50×50 mm pieces cut from 22 μm-thick amorphous Metglas 2705M ribbon. A miniature magnetoresistive probe is also shown that includes a KMZ10A magnetoresistive bridge and AMP04 instrumentation amplifier.

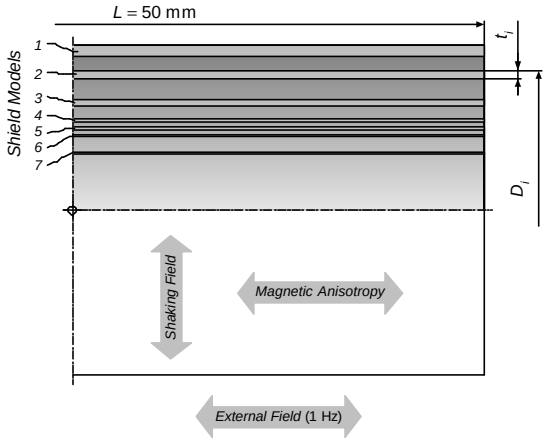

Fig. 4. Experimental shield models. (The models are shown as a coaxial assembly, although each cylinder was examined separately as a single-shell shield.) This figure illustrates that the thickness of each cylinder is directly proportional to its diameter, thus, keeping a constant t/D=1/45.5 ratio for all the models.

TABLE I
Experimental Shield Models
(L=50 mm, t/D = 1/45.5)

Shield Model	1	2	3	4	5	6	7
D_i, mm	20	16.1	13.1	11.1	10	8.9	7.1
t_i, μm	440	354	288	244	220	196	156
L/D_i	2.5	3.1	3.8	4.5	5	5.6	7

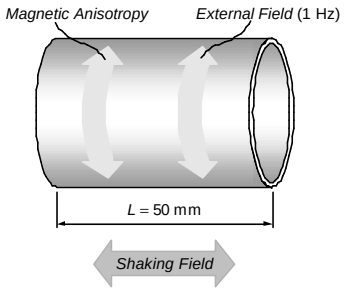

Fig. 5. Permeability measurement: the applied fields and magnetic anisotropy arrangement imitate the case of axial shielding. Low-frequency, 1 Hz, external field was applied by a toroidal coil wound around the shield. Magnetic induction was measured by another, separate toroidal coil. High-frequency, 1 kHz, shaking field was applied by a solenoid. Field magnitudes correspond to those used for measuring the axial shielding factor (Table. II).

1 Hz. At this frequency and for the highest $m=1.274\times10^6$ reached in the experiments, the penetration depth, 0.51 mm, for Metglas 2705M exceeds the thickness of the thickest shield (model No. 1 in Table I). Hence, all the axial shielding factors were measured nearly their static values [7].

We used a Helmholtz coil pair in order to apply the external 1-Hz magnetic field. The coils axis was set along the Earth's magnetic field. Another, coaxial Helmholtz coil pair was used to compensate the Earth's magnetic field. Each shield was demagnetized before the experiments. Shaking current [5] in the toroidal coils wound on the shields was supplied by a low-output-impedance power amplifier connected to an oscillator. The axial shielding factors were measured at the shields' center for different conditions described in Table II.

Fig. 6 shows a comparison between the experimental and theoretical results. The solid lines in this figure correspond to the effective shielding factor for an open axial shield [7]

$$\frac{1}{S_{ax\,eff}}=\frac{1}{S_{ax}}+\frac{1}{S_{ax\,op}},\ S_{ax\,op}\Big|_{t<<D}\approx\frac{1}{2.6\sqrt{L/D}}e^{k_L L/D}, \quad (4)$$

where $S_{ax\ op}$ is the axial shielding factor due to the openings and k_L is the axial exponential factor. The difference in the behavior of the solid and dashed characteristics is due to the substitution in (4) S_{ax} according to (2) with N_d^{rod} rather than with N_d^{ell} and the theoretically predicted k_L=2.405 [7] rather than the experimental k_L=2.26 [7].

One can see from Fig. 6 that the effect of the openings dominates for relatively short shields, with aspect ratios below 5, and is minor for relatively long shields, with aspect ratios beyond 5. It is important to note that in both these regions the experimental data is better approximated by (4) where the N_d^{rod} and k_L=2.405 are used.

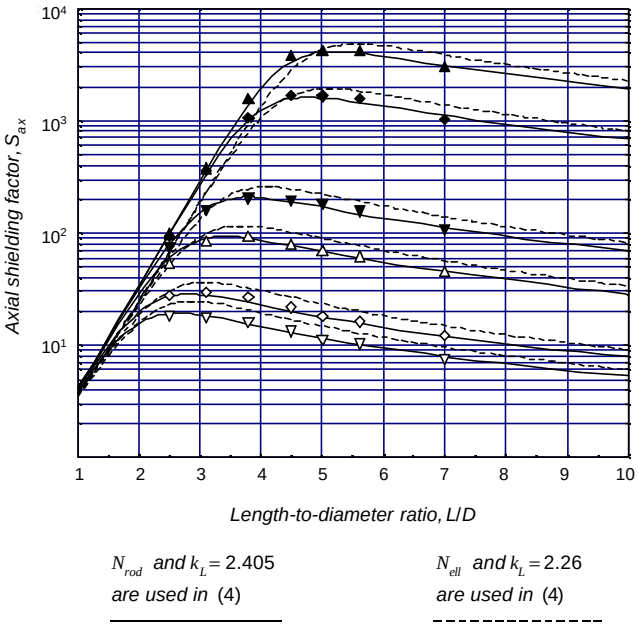

Fig. 6. Axial shielding factor of open cylindrical shields as function of their aspect ratio, *L/D*: a comparison between the experimental and theoretical results. This figure shows that the experimental data is better approximated by (4) where the demagnetizing factor for rod rather than for ellipsoid is used.

TABLE II
EXPERIMENTAL DATA

Data (see Fig. 6)	Shaking field (1 kHz), A/m	External field (1 Hz), mOe	Normalized permeability, mt/D
▲	30	300	28000
◆	15	300	10000
▼	5	300	1000
△	0	300	400
◇	0	100	100
▽	0	3	62

III. CONCLUSIONS

Axial shielding efficiency of open cylindrical magnetic shields is studied experimentally in a wide range of the shields length-to-diameter ratio (from 2.5 to 7) and in a wide range of the normalized permeability, mt/D, (from 62 to 28000). The experimental results suggest that axial shielding equations (2) and (4) should be corrected. A better matching between the theoretical and experimental results is achieved when the demagnetizing factor calculated for the equivalent rod rather for ellipsoid is substituted in (2) and the theoretically obtained in [7] k_L=2.405 rather than the experimental k_L=2.26 is substituted in (4).

ACKNOWLEDGEMENT

The support of the Ivanier Center for Robotics Research is gratefully acknowledged.

REFERENCES

[1] A. Mager, "Der magnetostatische längenabschirmfaktor von zylinderförmigen abschirmungen," *ETZ-A*, vol. 89, pp. 11–14, 1968.

[2] M. Kobayashi, and Y. Ishikawa, "Surface magnetic charge distribution and demagnetizing factors of circular cylinders," *IEEE Trans. Magn.*, vol. 28, pp. 1810–1814, 1992.

[3] E. Paperno, H. Koide, and I. Sasada, "A new estimation of the axial shielding factors for multishell cylindrical shields," *J. Appl. Phys.*, vol. 87, pp. 5959–5961, 2000.

[4] T. J. Sumner, J. M. Pendlebury, and K. F. Smith, "Conventional magnetic shielding," *J. Phys. D: Appl. Phys.*, vol. 20, pp. 1095–1101, 1987.

[5] E. Paperno and I. Sasada, "Effect of magnetic anisotropy on magnetic shaking," *J. Appl. Phys.*, vol. 85, pp. 4645-4647, 1999.

[6] I. Sasada, S. Kubo, and K. Harada, "Effective shielding for low-level magnetic fields," *J. Appl. Phys*., vol. 64, pp. 5696–5598, 1988.

[7] A. Mager, "Magnetic shields," *IEEE Trans. Magn*., vol. 6, pp. 67–75, 1970.